# Project 095 Assessment of Fuel Cells for Powering Modern Business Jets

## Georgia Institute of Technology

## Project Lead Investigator

Professor Dimitri N. Mavris
Director, Aerospace Systems Design Laboratory
School of Aerospace Engineering
Georgia Institute of Technology
Phone: (404) 894-1557
Fax: (404) 894-6596
Email: dimitri.mavris@ae.gatech.edu

## University Participants

**Georgia Institute of Technology (Georgia Tech)**

- P.I.: Dr. Dimitri N. Mavris
- FAA Award Number: 13-C-AJFE-GIT-158
- Period of Performance: March 19, 2024, to September 30, 2025
- Tasks:
  1. Developing a baseline vehicle model of the Gulfstream G280 aircraft
  2. Creating an off-line Proton Exchange Membrane Fuel Cell (PEMFC) system model that incorporates all aspects of fuel cell systems
  3. Integrating PEMFC model into the baseline aircraft model and conduct a trade study to identify promising opportunities for fuel cells to displace traditional systems

## Project Funding Level

This research was funded by the Federal Aviation Administration (FAA) Office of Environment and Energy through ASCENT, the FAA Center of Excellence for Alternative Jet Fuels and the Environment, Project 095 through FAA Award Number 13-C-AJFE-GIT-A95 under the supervision of Joshua Glottmann. Any opinions, findings, conclusions or recommendations expressed in this material are those of the authors and do not necessarily reflect the views of the FAA.

The FAA provided $200,000 in funding to Georgia Tech. Georgia Tech has secured in-kind cost share from both Gulfstream and Honeywell in the amount of $100,000, respectively, totally $200,000.

## Investigation Team

Dr. Dimitri Mavris, Georgia Tech, Principal Investigator
Dr. Jimmy C. Tai, Georgia Tech, Co-Principal Investigator
Mr. Berkay Terzi, Graduate Student Researcher, Georgia Tech (Task 2 and 3)
Mr. Jeremy Decroix, Graduate Student Researcher, Georgia Tech (Task 1, 2 and 3)
Mr. Leo Wattebled, Graduate Student Researcher, Georgia Tech (Task 2 and 3)
Mr. Axel Jazzini, Graduate Student Researcher, Georgia Tech (Task 2 and 3)

## Project Overview

The purpose of this research project is to identify opportunities for utilizing fuel cells on regional jet class aircraft to displace traditional power systems and reduce the total fossil fuel consumption of these vehicles. Fuel cell modeling and simulation will be performed for integration alongside an appropriate regional jet aircraft model.

# Task 1 – Developing a Baseline Vehicle Model

**Georgia Institute of Technology**

## Objective

The objective of Task 1 is to model and calibrate a notional Gulfstream® G280 aircraft model powered by a notional HTF7250G engine model and a GTCP36-150 auxiliary power unit (APU). The modeling and simulation environment used for this task is the Environmental Design Space (EDS). The notional aircraft model is calibrated against publicly available data.

## Research Approach

The notional G280 aircraft calibration process is performed using EDS and the results are validated against public available data from Gulfstream and the European Union Aviation Safety Agency (EASA) (EASA, 2020).

EDS is an aircraft modeling and simulation environment developed by Georgia Tech and based on validated National Aeronautics and Space Administration (NASA) software tools, e.g., FLight Optimization System (FLOPS), Weight Estimation for Turbine Engines (WATE++), and Numerical Propulsion System Simulation (NPSS) (refer to Figure 1). EDS was used to develop physics-based model of the G280 aircraft (see Figure 2), so that a parametric approach can be used to evaluate the effects of various design parameters. Built on the NPSS object-oriented framework, EDS supports automated data exchange between modules, allowing for comprehensive analysis of engine architectures and airframe configurations, including multi-design point cycle designs. The comprehensive suite of software tools which comprise EDS are integrated and designed to enable a thorough assessment of the environmental impacts associated with aviation.

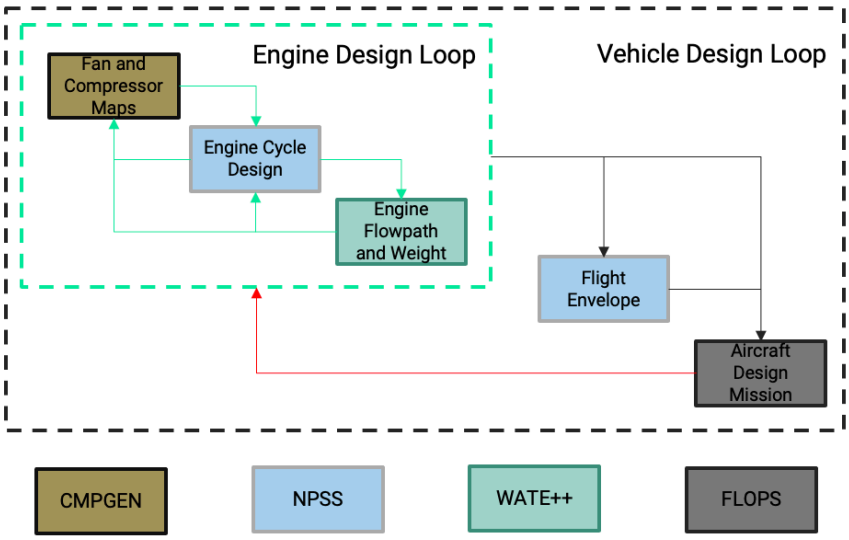


**Figure 1.** Environmental design space vehicle design loop. FLOPS: FLight Optimization System; NPSS: Numerical Propulsion System Simulation; and WATE++: Weight Estimation for Turbine Engines.

® Gulfstream is a registered trademark of Gulfstream Aerospace Corporation, Savannah, Georgia


**Figure 2.** Gulfstream G280 business jet.

The Gulfstream G280 is a super mid-size business jet designed and manufactured jointly by United States (U.S.)-based Gulfstream Aerospace and Israel Aerospace Industries. The G280 is equipped with two Honeywell® HTF7250G engines with a rated takeoff thrust of 7,624 lbf each. The notional HTF7250G mixed flow turbofan engine model was sized using the multi design point (MDP) methodology and calibrated using International Civil Aviation Organization (ICAO) databank to match the thrust-specific fuel consumption (TSFC) at four different sea level static (SLS) uninstalled points: take-off, climb-out, approach and idle. The results of the very close calibration are shown in Figure 3.

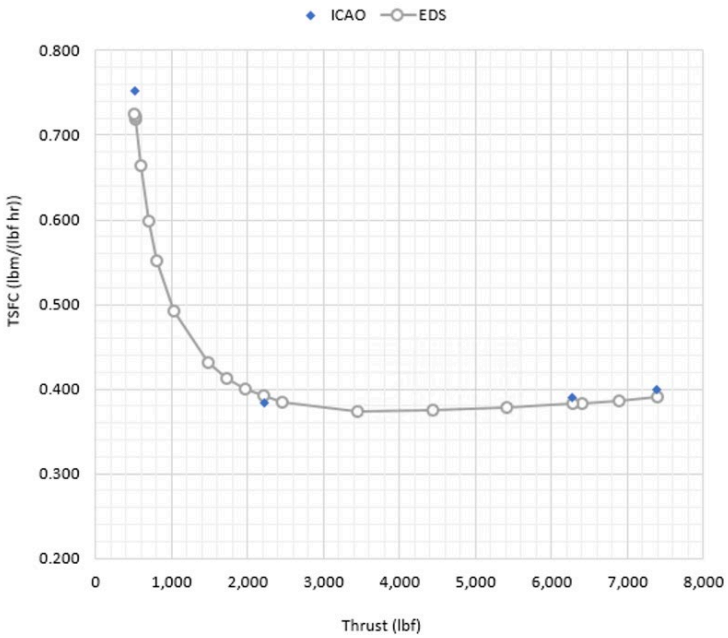


**Figure 3.** Environmental Design Space (EDS) HTF7250G engine calibration using International Civil Aviation Organization (ICAO) databank.

The APU being displaced onboard of the aircraft during this research effort is the GTCP36-150. Figure 4 outlines the key performance data for the GTCP36-150. It has a single-stage centrifugal compressor and a single-stage radial turbine architecture. Its weight varies between 125 lb (51 kg) and 168 lb (76 kg) depending on the standard and high flow rates. With the integration of a k-factor of 2.2, the group weight value of 370 lb (168 kg) can be obtained. The rated horsepower can go up to 40kVA (59 F, SL) and the bleed airflow goes up to 70lb/min (59 F, SL). The rotor speed ranges from 58,737 to 62,000 rpm with a maximum operating altitude of 20,000 ft (Honeywell, 2008).

® Honeywell is a registered trademark of Honeywell International, Inc., in the United States and other countries.

**Key Performance Data**

| | |
|---|---|
| Weight: | 125 – 168lbs |
| Digital Control Weight: | 6lbs |
| Basic Spec: | FAA TSO-C77a Category 1 (Essential) |
| Rated Horsepower: | Up to 40kVA, 59F, SL |
| Bleed Airflow: | Up to 70lb/min, 59F, SL |
| Rated EGT: | 1230F |
| Rotor Speed: | 58,737 – 62,000 rpm |

**Figure 4.** APU GTCP36-150 characteristics (Honeywell, 2008). EGT: exhaust gas temperature.

The role of the APU is to provide electrical and pneumatic power to the aircraft during the ground operations while the engines are turned off. Its role can also be to start the main engines. After the main engines start, the APU system is turned off. In case of an engine failure, the APU will be turned on after an emergency descent under 20,000 ft. For on the ground operations, if the APU is running for an hour, assuming a fuel consumption of 231 lb/hr (104 kg/hr) it will consume 231 lb (105 kg) of fuel before the taxi out segment.

Using the previous technical specification of the G280 found in Tables 1 and 2 and leveraging the engine deck of the notional HTF7250G mixed flow turbofan engine model, the notional G280 model was calibrated by performing a mission analysis with the FLOPS software. FLOPS takes the statistical weights fractions of each subsystem on the aircraft as input, the geometry of the aircraft from the computer aided design three-dimensional view rendering and the payload and range values.

**Table 1.** G280 aircraft specifications.

| G280 Aircraft Specifications | |
|---|---|
| **Overall Wingspan** | 63 ft |
| **Fuselage Length** | 66.8 ft |
| **Fuselage Height** | 11.2 ft |
| **Fuselage Width** | 7.9 ft |
| **Passenger Compartment Length** | 25.8 ft |
| **Maximum operating Mach number** | 0.85 |
| **Long Range Cruise Mach Number** | 0.8 |
| **Maximum Cruise Altitude** | 45,000 ft |
| **Maximum Range** | 3,600 nmi |
| **Passenger** | 4 |
| **Crew Member** | 2 |

**Table 2.** Notional G280 model detailed weight breakdown. EDS: Environmental Design Space.

| Mass Breakdown | Reference (lb) | EDS Results (lb/kg) | Error (%) |
|---|---|---|---|
| **Auxiliary Power Unit** | 252 (114) | 252 (114) | 0 |
| **Operating Empty Weight** | 24,150 (10,954) | 24,151 (10,955) | 0.004 |
| **Maximum Payload** | 1,000 (454) | 1,000 (454) | 0 |
| **Mission Fuel Weight** | 14,600 (6,622) | 14,601 (6,623) | 0.007 |
| **Ramp Weight** | 39,750 (18,030) | 39,752 (18,031) | 0.005 |
| **Taxi Out Fuel** | 150 (68) | 151 (68) | 0.67 |
| **Maximum Takeoff Weight** | 39,600 (17,962) | 39,601 (17,963) | 0.003 |
| **Design Landing Weight** | 32,700 (14,832) | 32,703 (14,834) | 0.009 |

The baseline calibration was performed using the maximum payload (1,000 lb/454 kg) and the maximum mission fuel weight (14,600 lb/6,622 kg) for the maximum range (3,600 nmi) with a reserve mission of 30 minutes at 10,000 ft. A cruise climb schedule was implemented. The results of the calibration show a very close percentage error for the aggregated weights as indicated in Table 2.

### Milestones

- Performed calibration of the notional HTF7250G engine model.
- Performed calibration of the notional G280 aircraft model.

### Major Accomplishments

Performed the notional baseline aircraft model of the G280 super mid-size business jet which allowed for the integration of the PEMFC system impact.

### Publications

None.

### Outreach Efforts

- Scheduled and participated in monthly meetings with Gulfstream, Honeywell, and FAA to guide this research effort.
- Attended ASCENT biannual meetings.

### Awards

None.

### Student Involvement

This task involves one graduate student, Jeremy Decroix (PhD candidate). He is in charge of the notional HTF7250-G engine model and the G280 notional baseline aircraft model calibration against publicly available data.

### Plans for Next Period

Continue to refine the mission schedule used for the calibration to make sure the integration of the PEM fuel cell system is accurate.

## Task 2 – Creating Off-line PEMFC System Model

**Georgia Institute of Technology**

### Objective

The objective of this task is to develop a comprehensive modeling and simulation environment for fuel cells, with potential application in the target aircraft. After evaluating traditional power system alternatives for APUs, Solid Oxide Fuel Cells

(SOFCs) and Proton Exchange Membrane Fuel Cells (PEMFCs) emerge as the most promising options (Daggett et al., 2003). Given PEMFCs' lower operating temperature, high efficiency, and their power output profiles that align with the typical power demands of business jets, PEMFCs are considered the preferable option for APU applications in business jets. Therefore, the modeling and simulation environment developed in this task will focus on PEMFC technology.

## Research Approach

Designing a novel power system for an aircraft demands a comprehensive understanding of both onboard power sources and aircraft system-level power demands. In conventional aircraft, gas turbine engines generate electrical power via generators connected to the engine spools and supply bleed air for the environmental control system (ECS). Additionally, traditional APUs provide electrical power and bleed air during ground operations, engine start-up, and in certain emergency scenarios. For a fuel cell system to feasibly replace a gas turbine APU, it must at least fulfill all these operational requirements which are namely, supplying electrical power to onboard subsystems, delivering pressurized air for the ECS, and supporting engine start-up without relying on ground power units.

Although a fuel cell system can be sized to meet the original requirements of a conventional APU, an alternative approach involves adjusting these requirements to better align with the benefits offered by emerging aircraft systems. This strategy serves as a step toward achieving a More Electric Aircraft. In this configuration, the fuel cell system is designed to supply continuous electrical power and pressurized air to the ECS throughout the entire flight, rather than being limited to ground operations and emergency situations. By enabling these capabilities, the approach aims to reduce Jet-A fuel consumption and lower overall emissions by eliminating the need for customer bleed air and shaft power extraction from the main engines.

To successfully replace the gas turbine APU with a fuel cell system under a revised mission profile, the system must operate reliably across a wide range of environmental conditions, including hot- and cold-day ground operations, takeoff, and high-altitude flight. For instance, during hot-day scenarios, the ambient air drawn into the cooling ducts by fans may reach such high temperatures that the temperature differential between the air and the fuel cell stack becomes minimal. This necessitates a significantly larger volume of cooling air, often exceeding the capacity of conventional ducting systems. In such cases, advanced cooling cycles may be required to meet thermal management demands (Bargal et al., 2020). In contrast, during cold-day operations, the primary challenge becomes preheating the intake air before it enters the fuel cell stack to maintain optimal performance.

The capability to operate at high altitudes presents significant challenges for the proposed fuel cell system, primarily due to the low ambient pressure at such elevations. For air-breathing fuel cells, reduced pressure directly impacts performance by lowering the open-circuit voltage (Willich et al., 2014), as shown in the Nernst equation through the partial pressure of hydrogen. Additionally, low pressure adversely affects activation and concentration overpotentials and indirectly increases ohmic overpotential (Willich et al., 2024). Therefore, incorporating compression elements upstream of the fuel cell is essential to ensure efficient performance at high altitudes. However, these compression components require power to operate and to achieve a self-sustained fuel cell system, this power should be supplied by the fuel cell stacks themselves.

Modeling the stack-level performance of a low-temperature PEMFC alone is insufficient for making informed aircraft-level design decisions, especially during the early stages of conceptual development. This is primarily because the balance of plant (BoP) components in a low-temperature PEMFC system (e.g., compressors, pumps, and thermal management subsystems) are significant electrical consumers. These components contribute to the parasitic power load, directly impacting the system's net electrical output available to serve onboard loads such as avionics, galleys, and other aircraft subsystems. Therefore, a complete system-level model that includes both the fuel cell stack and auxiliary components is essential to establish a robust, parametric simulation environment.

The proposed PEMFC system is designed to replace the conventional gas turbine APU while ensuring continuous and reliable power delivery to all aircraft subsystems throughout the flight, in accordance with the defined sizing mission. The overall aircraft system architecture is illustrated in Figure 5. The BoP for the fuel cell system can be divided into three primary subsystems: the air supply system, the fuel conditioning system, and auxiliary components.

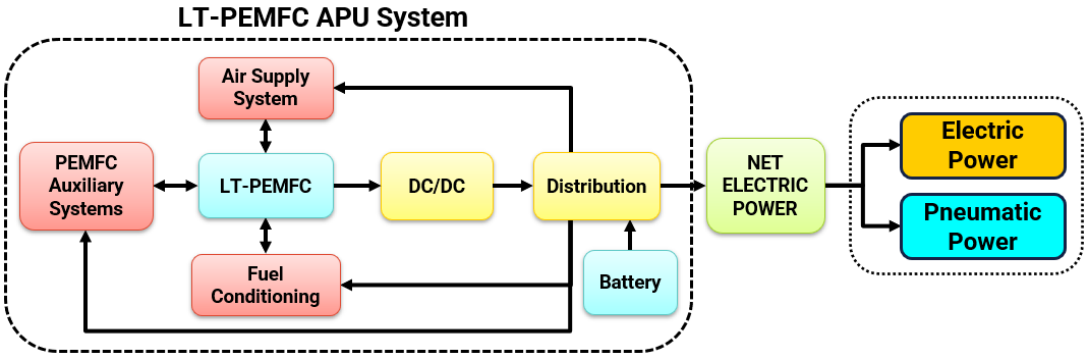


**Figure 5.** General overview of the proposed power system. APU: auxiliary power unit, LT-PEMFC: Low-Temperature Proton Exchange Membrane Fuel Cells, and DC: direct current.

One of the main objectives of this task is to quantify the parasitic power demands, or in other words, the power requirements of the auxiliary components in the PEMFC system. As illustrated in Figure 5, the power sources for the auxiliary components include both the PEMFC stack and a parallel battery. The battery serves as an additional power source to assist the fuel cell stack during rapid transients in power demand, periods of high-power demand, or emergency situations. The outputs of the proposed system include direct current (DC) electrical power for use in aircraft subsystems and pressurized air for the aircraft's ECS.

The air supply subsystem is responsible for delivering the required mass flow of air at the appropriate pressure and temperature to the PEMFC stacks. The fuel conditioning subsystem regulates the flow of hydrogen to the stacks, ensuring optimal electrochemical performance. The auxiliary subsystem includes supporting components such as heat exchangers for thermal management, as well as controllers, valves, and various monitoring devices. The net electrical output of the system, after accounting for parasitic power consumption by auxiliary subsystems, is available to supply the aircraft's electrical loads and to generate pneumatic power for the ECS.

The mechanical system architecture, illustrated in Figure 6, is designed to ensure reliable operation of the PEMFC under a wide range of flight conditions, including high-altitude environments where ambient air pressure and density are significantly reduced. In such scenarios, ambient air must first be compressed to meet the stack's pressure requirements. This compression process raises the air temperature above the optimal operating range for the fuel cell, necessitating the use of a heat exchanger to cool the air before it enters the stack. Subsequently, a humidifier adjusts the humidity of the air, utilizing the system's by-product water to meet the fuel cell's specific moisture requirements.

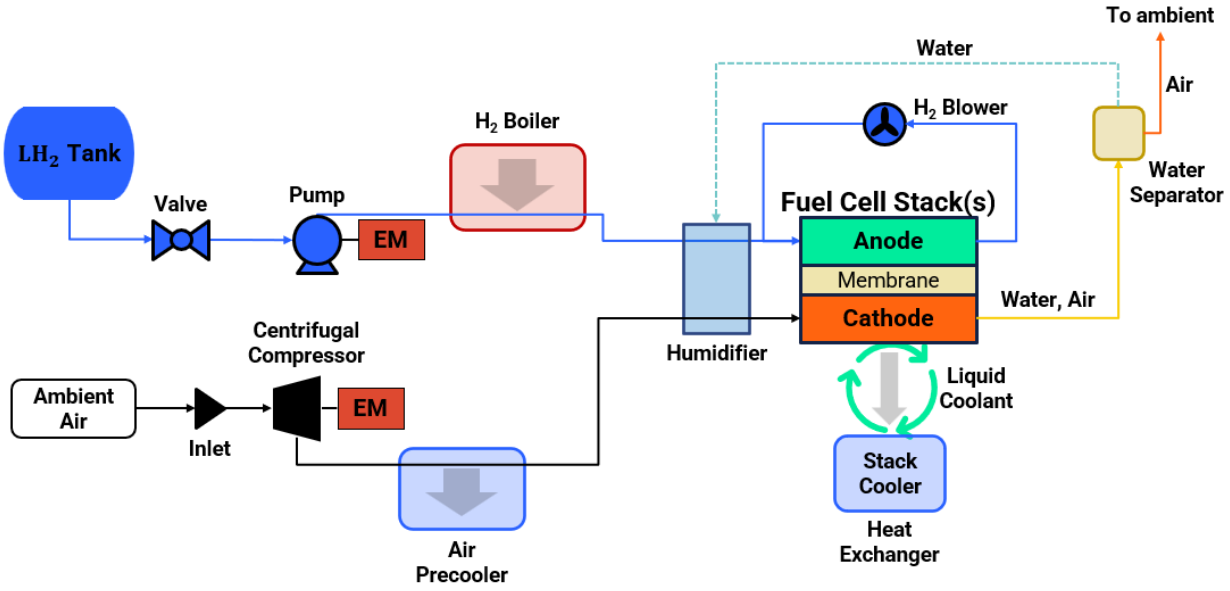


**Figure 6.** Fuel cell system architecture.

PEMFCs require high-purity hydrogen, as they are highly sensitive to contaminants. While hydrogen can be stored in either gaseous or liquid form, liquid hydrogen is often preferred due to its superior gravimetric energy density. However, storing cryogenic hydrogen onboard presents thermal and mechanical challenges. The storage tank must be designed to minimize heat ingress from the environment. Before delivery to the stack, the liquid hydrogen is gasified and heated to the required temperature using heat exchangers. Because of the low mass flow rates involved, pressurization is achieved using micropumps. Any excess hydrogen is recirculated back into the system via a blower to improve efficiency and maintain consistent fuel supply.

Inside the PEMFC stack, the electrochemical reaction is exothermic, generating substantial heat energy. To maintain the stack within its optimal operating temperature range, typically between 20°C and 90°C, a closed-loop single-phase liquid cooling system is used. This system includes a liquid-cycle heat exchanger that effectively dissipates the waste heat, ensuring stable and efficient stack performance under varying operational conditions.

As shown in Figure 5, the pneumatic power, i.e., the compressed air supplied to the ECS, is one of the two outputs of the new APU system. In aircraft, the ECS is responsible for maintaining a safe and comfortable cabin environment by regulating pressure, temperature, and humidity. Traditionally, engine bleed air serves as the primary airflow source for the ECS. The system typically includes two pneumatic air conditioning kits, commonly referred to as packs, which manage core air conditioning and distribution functions. A schematic of this traditional configuration is shown in Figure 7.

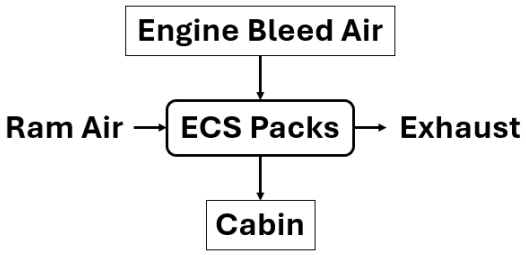


**Figure 7.** Conventional environmental control system (ECS) schematic (Cai, 2023).

As this project investigates the transition toward more electric aircraft architecture, electrifying the ECS using power supplied by a fuel cell system offers a promising opportunity to reduce Jet-A fuel consumption by minimizing reliance on engine bleed air. Therefore, accurately quantifying the power consumption, as well as other key parameters (e.g., weight and ram airflow) of the electrical environmental control system (eECS) is essential for the proper sizing of the fuel cell system. To accomplish this, defining the new eECS architecture is a key step. The cabin air compressor system consisting of centrifugal compressors and their associated drive mechanisms represents one of the major modifications to the ECS and serves as a primary power consumer. A general schematic of the eECS configuration is presented in Figure 8. Furthermore, trade-off studies can be conducted on the packs, which currently exhibit low efficiencies (Rosero et al., 2007), to evaluate their weight and performance for electrified applications, especially considering that the new cabin air compressor system may deliver cooler, lower-pressure air compared to traditional engine bleed air.

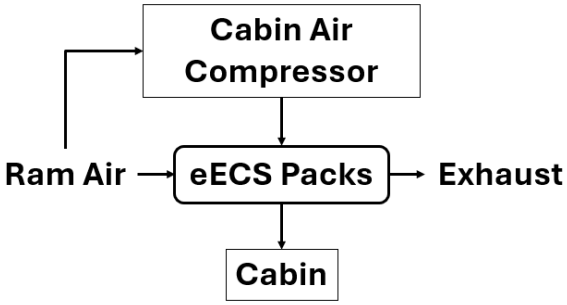


**Figure 8.** Electrical environmental control system (eECS) schematic (Cai, 2023).

When updating the aircraft's ECS, several key requirements must be met to ensure mission suitability. According to FAA regulations, the minimum airflow that must be supplied to the cabin is 0.55 lb/min per passenger (FAA, 1996). In addition to meeting this constraint, the system must deliver sufficient mass flow to refresh the cabin air within a defined time interval while maintaining a steady cabin temperature by effectively removing the internal heat load.

The modeling of the proposed system is carried out in the NPSS environment. NPSS is an object-oriented simulation platform primarily developed for modeling gas turbine engine cycles, but its modular structure also enables broader applications. The software provides a library of built-in components while offering flexibility to define custom elements and user-defined functions. This adaptability, combined with its robust numerical solver and support for multiple thermodynamic property packages, makes NPSS a powerful environment for system-level modeling. Its capability to simulate both on-design and off-design performance scenarios is particularly valuable for this study, as it supports accurate component sizing and performance assessment, which are key requirements for establishing a reliable parametric simulation framework. The fuel cell modeling process is divided into five main steps.

**Step 1: Baseline Flight Mission Definition and Design Point Selection**
Sizing a fuel cell system, including hydrogen storage and cabin air compressors, to continuously supply electrical power to aircraft subsystems and pressurized air to the eECS throughout the flight requires a well-defined aircraft mission, which must include a detailed profile of the electrical power requirements of the onboard systems. Although aircraft power demand profiles can sometimes be obtained directly from manufacturers, the study by Voth et al. (2024) presents a methodology to estimate the electrical power requirements of several aircraft subsystems. Additionally, a pack model incorporating the selected thermal conditioning strategy for the eECS must be included to determine air demand and the corresponding power consumption across the ground, flight, and reserve phases of the mission. A generic altitude profile for the baseline aircraft, which is considered in the sizing process, is shown in Figure 9. The flight mission is critical in determining the design point of the new system and in properly sizing the liquid hydrogen ($LH_2$) tank. For the design point of this project, the maximum possible altitude is selected, where the air density will be lowest for the given flight mission.

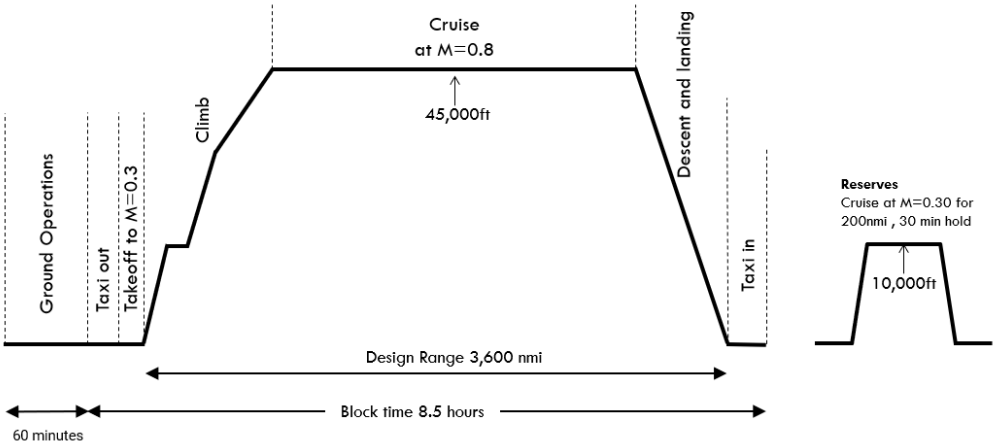


**Figure 9.** Baseline flight mission summary.

**Step 2: PEMFC Stack Sizing**

Fuel cell modeling approaches span from zero-dimensional to three-dimensional frameworks, with increasing fidelity and computational complexity. For early-stage aircraft design and system-level analysis, zero-dimensional and one-dimensional models are typically favored, as they provide sufficient accuracy with lower computational cost. In this project, a zero-dimensional empirical electrochemical model of a PEMFC is adopted, informed by various established references.

This model incorporates the three main voltage losses—activation, ohmic, and concentration—that reduce the actual output voltage from the theoretical maximum. The analysis begins by calculating the reversible cell voltage using the Nernst equation, which is a function of the stack temperature and the partial pressures of hydrogen, oxygen and water vapor. This reversible voltage represents the ideal open-circuit potential under given conditions. However, real-world performance is reduced due to inherent electrochemical and physical limitations (O'Hayre et al., 2016).

$$E_{rev} = E^{\circ} + \frac{\Delta \hat{s}}{nF}(T - T_0) - \frac{RT}{nF}\ln\left(\frac{p_{H_2O}}{p_{H_2} \cdot p_{O_2}^2}\right) \quad \text{(Eq. 1)}$$

The first category of voltage loss is activation loss, which dominates at low current densities. It is associated with the energy required to initiate electrochemical reactions at the anode and cathode. This loss is described using a modified form of the Tafel equation (O'Hayre et al., 2016):

$$E_{act} = -\frac{RT}{\alpha n_e F}\ln(i_0) + \frac{RT}{\alpha n_e F}\ln(i + i_{leak}) \quad \text{(Eq. 2)}$$

The second major source of voltage loss is the ohmic loss, which arises from resistance to charge transport within the fuel cell. This resistance primarily stems from proton transport through the polymer electrolyte membrane. The associated voltage drop is calculated using the area-specific resistance (ASR) of the membrane, which encapsulates the resistivity of the membrane as a function of its thickness, surface area, and proton conductivity (O'Hayre et al., 2016):

$$E_{ohm} = i \cdot ASR_{ohmic} \quad \text{(Eq. 3)}$$

The third loss mechanism is the concentration loss, which becomes prominent at high current densities. This loss results from limitations in mass transport, particularly the depletion of reactants near the catalyst layer or the accumulation of products that impede further reactions. As the fuel cell approaches its limiting current density, the reactant concentrations at the electrode surface tend towards zero, leading to a sharp increase in loss. The concentration overpotential is modeled by (O'Hayre et al., 2016):

$$E_{conc} = \left(1 + \frac{1}{\alpha}\right)\frac{RT}{n_e F}\ln\left(\frac{i_L}{i_L - (i + i_{leak})}\right) = \mathrm{C} \cdot \ln\left(\frac{i_L}{i_L - (i + i_{leak})}\right) \quad \text{(Eq. 4)}$$

By summing the activation, ohmic, and concentration losses and subtracting them from the reversible voltage, the effective output voltage of the PEMFC can be estimated as follows. This equation forms the foundation for assessing the performance of each cell in the stack.

$$E_{cell} = E_{rev} - (E_{act} + E_{ohm} + E_{conc}) \quad \text{(Eq. 5)}$$

Although this model is relatively simple, it depends heavily on design constants outlined in the governing equations. Datta (2021) provides these key constants across different pressure levels, as presented in Table 3. The same study also offers correction factors to account for variations in operating stack temperature and humidity, enabling more accurate modeling under diverse conditions.

**Table 3.** Model parameters used in PEMFC simulation (Datta, 2021). ASR: area-specific ohmic resistance.

| Pressure | 1 atm | 2 atm | 3 atm | 4 atm |
|---|---|---|---|---|
| $i_{0,C}$ | $10^{-4}$ | $10^{-4}$ | $10^{-4}$ | $10^{-4}$ |
| $\alpha_C$ | 0.15 | 0.155 | 0.155 | 0.16 |
| $i_{0,A}$ | 0.1 | 0.1 | 0.1 | 0.1 |
| $\alpha_A$ | 0.5 | 0.5 | 0.5 | 0.5 |
| $i_L\ (A/cm^2)$ | 0.73 | 1.0 | 1.1 | 1.23 |
| $i_{leak}\ (A/cm^2)$ | 0.01 | 0.01 | 0.01 | 0.01 |
| $C\ (V)$ | 0.08 | 0.08 | 0.08 | 0.12 |
| $ASR_{ohmic}\ (\Omega\ cm^2)$ | 0.12 | 0.115 | 0.1 | 0.06 |

To achieve the required electrical power output, individual fuel cells are connected in series to form a stack, thereby increasing the overall voltage. The total number of cells is determined based on the target stack and individual cell voltages, while the required membrane area is calculated from the desired stack-level current density. Under off-design conditions, although the physical dimensions of the stack (i.e., number of cells and membrane area) remain fixed, its performance varies with changes in aircraft altitude and speed. In addition to electrical power, fuel cell stacks produce waste heat, which can be repurposed for various onboard functions. Accurately quantifying this waste heat is critical for TMS sizing and is dependent on both cell efficiency and electrical power output.

$$Waste\ Heat = \left(\frac{1}{v} - 1\right) \times PWR_{cell} \quad \text{(Eq. 6)}$$

where $v$ is the cell efficiency and $PWR_{cell}$ is the electrical power generated by the cell.

To estimate the stack weight, Datta (2021) provides a detailed approach that accounts for individual sub-components. Alternatively, a simplified estimation can be made using a specific power-based method, in which the maximum stack power is divided by a representative specific power value. The Fuel Cell Roadmap report (Aerospace Technology Institute, 2022), prepared for FlyZero project, outlines specific power targets for future years. However, due to the relatively low Technology Readiness Level (TRL) of the system, there is considerable uncertainty in these values. To address this, confidence intervals should be established to capture the range of possible outcomes. Using the latter method, the fuel cell stack weight is estimated by dividing the maximum stack power—although potentially outside the typical operating range, as illustrated in the polarization curve in Figure 10, by an assumed specific power value.

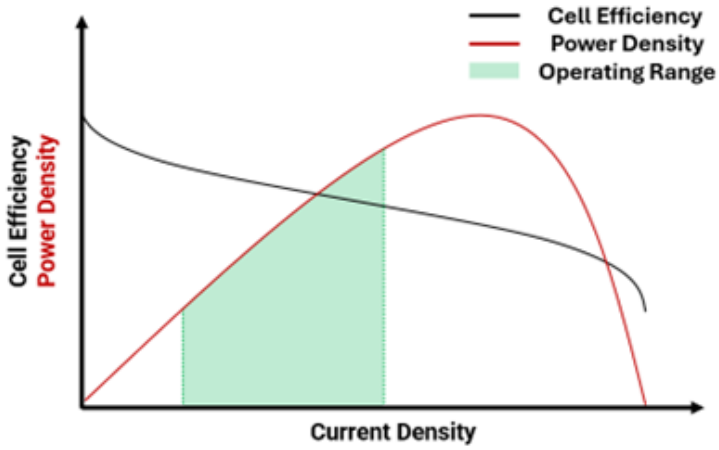


**Figure 10.** Cell efficiency and power density versus current density.

**Step 3: Balance of Plant Sizing and Modeling**
As illustrated in the fuel cell system architecture, the system comprises several auxiliary components, including pressure-boosting elements such as compressors and pumps. The fuel cell compressor and hydrogen micropump requirements are determined by the pressure and flow rate demands of the fuel cell stack at the selected design point. The most critical design condition corresponds to the maximum operating altitude of the baseline aircraft. From the stack perspective, specifying the stack design pressure and temperature is essential, as these parameters directly influence the compressor pressure ratios and overall stack performance.

The power requirement for the air compressor is calculated using the following relation with compressor efficiency. The total enthalpy rise and power without any bleed across the compressor is given by:

$$h_{t,out} = h_{t,in} \times \left[1 + \frac{\left(\Pi_{cmp}^{\frac{\gamma-1}{\gamma}} - 1\right)}{\eta_{\text{cmp}}}\right] \quad \text{(Eq. 7)}$$

$$PWR_{cmp} = \dot{W}_{cmp} \times \left(h_{t,in} - h_{t,out}\right) \quad \text{(Eq. 8)}$$

where $\Pi = \frac{p_{t,\text{out}}}{p_{t,in}}$ is the total pressure ratio across the compressor, $\dot{W}_{cmp}$ is the mass flow rate through the compressor, and $\gamma$ is the specific heat ratio of air.

To accurately quantify the power consumption of the cabin air compressor system, which comprises multi-stage centrifugal compressors, an electric motor, and associated components required for motor operation, in the eECS, additional system details must be defined. As proposed by Tagge et al. (1985), the system may be configured with three cabin air compressors: two dedicated to normal operation and one serving as a redundant unit for emergency situations. The overall system architecture is illustrated in Figure 11. Depending on the number of packs implemented, the total number of compressors, as well as the allocation between operational and backup units, may vary.

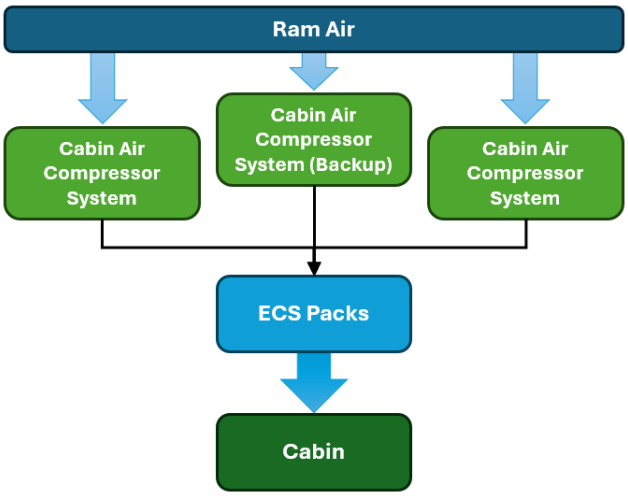


**Figure 11.** Overall electric environmental control system (eECS) system architecture.

Tagge et al. (1985) also presented several system configurations in their study, each employing a different thermal conditioning method, namely, air-cycle, vapor-cycle, and air-cycle with heat exchanger cooling. The selected thermal conditioning approach significantly influences the discharge pressure requirements of the cabin air compressors, which in turn directly impacts their power consumption, as illustrated in Figure 12. For instance, implementing a vapor-cycle system can lead to substantial reductions in compressor power consumption due to its lower discharge pressure requirement. However, since this approach alters the thermal management architecture, its broader implications must be carefully evaluated through detailed system-level analysis to ensure overall performance and integration benefits.

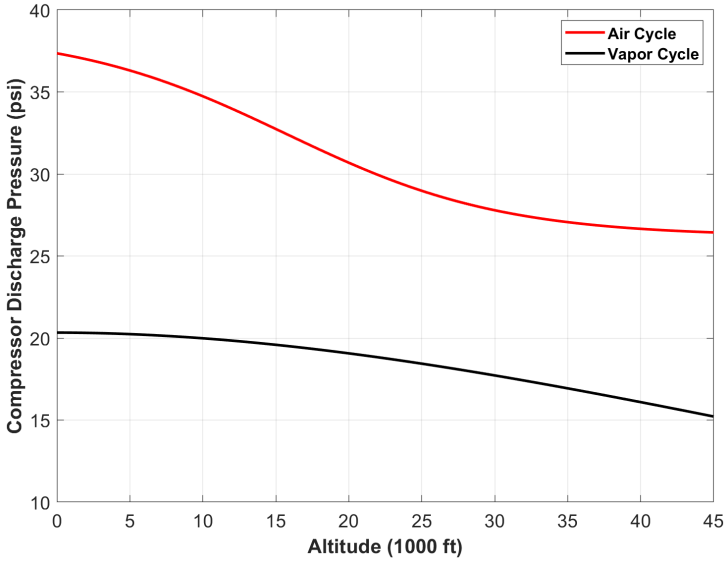


**Figure 12.** Required discharge pressure of cabin air compressors as a function of altitude (Tagge et al.,1985).

Another important consideration for the turbomachinery is the weight estimation for each of the components. In the case of this study, centrifugal compressors are selected over axial compressors. Indeed, axial compressors are known for higher efficiency and handling larger mass flows and thus will be privileged for big jet engines applications. Centrifugal

compressors, on the other hand, have higher compression per stage, are more compact and are easy to maintain (Campbell & Talbert, 1945). Therefore, they are more suited in the case of this study.

To estimate the weight of the ECS and fuel cell compressors, the needed inputs for both are the maximum required mass flow rate as well as the maximum pressure ratio. These values can be obtained through the modeling and simulation environment previously described. They are then compared to the values of existing compressors from manufacturers' databases available online and a suitable solution is determined, and the weight of the selected industrial solution is used.

With a similar approach, the design pressure ratio for the hydrogen pump is estimated by considering liquid hydrogen tank pressure and pressure losses across the hydrogen boiler to ensure that hydrogen is delivered to the stack at the required pressure. The hydrogen pump shaft power is then calculated as the product of the volumetric flow rate and the pressure difference, divided by the pump's hydraulic efficiency, representing the hydraulic power requirement:

$$PWR_{pump} = \frac{Q \times \Delta P}{\eta_{pump}} \quad \text{(Eq. 9)}$$

Efficiencies are critical factors in calculating the performance of both compressors and pumps. Performance maps, sourced either from manufacturers or derived from semi-empirical models in turbomachinery literature, are used to evaluate these components under off-design conditions. These maps are then scaled according to the specified on-design efficiency to estimate power requirements during off-design operation.

For the hydrogen pump, the choice to use a micropump is made. Indeed, the required hydrogen mass flow rate required by the stack will remain very low. The exact value can be determined in the modeling and simulation environment that was developed for this study. The weight estimation is then obtained by following the exact same methodology as for the ECS and fuel cell compressors. Manufacturers databases are analyzed, and the weight of a suitable industrial solution is used.

Another important BoP subsystem is the electrical components, which include but are not limited to electric motors, power converters, and batteries. Among these components, electric motors serve as the backbone of fuel cell systems, converting electrical power generated by the fuel cell into mechanical power to drive key components such as compressors. Depending on system requirements, various motor types can be employed, including brushless DC motors (MicroPump, Inc., 2025) and permanent magnet synchronous motors (Rotrex Fuel Cell Compressors, 2025). Motor sizing is based on the mechanical power demands of the fuel cell system and accounts for the projected design efficiency. Pastra et al. (2022) provide efficiency and specific power projections for electric motors in future years, which are used as reference points. Once the motor is sized, shaft power output is evaluated using an efficiency map derived from industrial motor data, scaled to reflect the chosen design-point efficiency.

Alongside electric motors, power converters play a crucial role in the electrical BoP by ensuring that the electrical power from the fuel cell is properly conditioned to meet the voltage and current requirements of the system. For example, a DC-DC converter is required to regulate the output voltage of the fuel cell stack to match the bus voltage, which is determined primarily by the aircraft subsystem requirements and the battery voltage. This converter ensures stable and consistent DC output. Additionally, since electric motors within the fuel cell system require alternating current (AC) input, DC-AC inverters are employed to convert the regulated DC voltage into AC. Similar to electric motors, the design efficiency of these power electronics components is critical. Hall et al. (2022) provide projections for future years, including efficiency targets and specific power values, which inform the sizing and performance assessment of these devices.

In the proposed system architecture, the secondary energy storage device, the battery, plays a critical role in supporting the fuel cell system by fulfilling several essential functions. At startup, it supplies electrical power to the balance-of-plant components, such as electric motors driving the compressors and temperature regulation units for air and hydrogen, enabling the system to initiate autonomously without external power. Once the PEMFC stack generates sufficient power to cover parasitic loads and provide a net output to aircraft subsystems, the battery can be deactivated. Additionally, due to the inherently slow dynamic response of fuel cell systems to transient power demands, the battery also acts as a buffer to manage power fluctuations, ensure consistent system output, and supplement the fuel cell during peak load conditions (Smith et al., 2021). In this setup, the fuel cell is sized to meet average power requirements, while the battery handles dynamic variations. Future projections for battery specific energy and associated confidence intervals are provided by Tiede et al. (2022), offering valuable input for long-term planning.

The water management system is designed to control the fuel cell's humidity, which directly affects the membrane's resistance. Therefore, the humidity levels of fuel cell must be carefully controlled throughout the flight mission, regardless of environmental conditions. To maintain appropriate humidity levels, the system may utilize the by-product water generated during fuel cell operation, enabling a more self-sustained configuration. This water can be collected via a water separator and subsequently directed to the humidifier, while any excess water can be expelled into the atmosphere.

Various types of humidification systems are available for fuel cell applications, with membrane humidifiers and enthalpy wheels being the primary options (Chang et al., 2018). Since enthalpy wheels require electrical power to operate, membrane humidifiers are generally considered a more efficient solution for this application.

For weight estimation of the humidification system, industrial data can be used to develop a simple parametric model. For example, Schröder et al. (2021) estimate the weight of a membrane-type humidifier based on the dry air mass flow rate that supplied to the stacks, using a value of 82.353 kg/(kg/s of dry air). The weight of the water separator is typically negligible compared to that of the humidifier, as indicated by the industrial supplier (MANN+HUMMEL, n.d.).

**Step 4: Liquid Hydrogen Tank Sizing**
After sizing all components of the fuel cell system and finalizing the design, the total hydrogen fuel required for the complete sizing mission, including reserve segments, is calculated. Based on this estimated total hydrogen consumption, the hydrogen storage tank is sized. It is assumed that a single storage tank is placed within the fuselage, designed as a cylindrical vessel with 2:1 semi-ellipsoidal heads. Due to the significantly higher ambient temperature in the fuselage compared to the cryogenic storage temperature of liquid hydrogen, a constant inward heat flux occurs during flight. This heat is absorbed by both the liquid and gaseous hydrogen, accelerating the boil-off phenomenon. To mitigate hydrogen losses, the tank is equipped with an insulation jacket. For the sizing process, the choice of tank and insulation material is critical, as both heat transfer characteristics and structural weight must be carefully balanced. In a study conducted by Johnson et al. (2024), candidate tank materials such as aluminum alloy Al 5083 (a metallic option) and Cycom® 5320 (a composite material), along with various insulation materials, were evaluated. Among these, the combination of Cycom 5320 with a Quest® vacuum insulation jacket provided the best performance in terms of thermal insulation and overall weight efficiency. The material properties of these materials are summarized in Table 4.

**Table 4.** Material properties for hydrogen tank design (Johnson et al., 2024).

| Properties of Cycom5320 | | Properties of Quest Vacuum Jacket | |
|---|---|---|---|
| Property | **Value** | **Property** | **Value** |
| **Yield Stress [psi]** | 190,000 | Density [kg/m$^3$] | 0.0 |
| **Density [kg/m$^3$]** | 1,310 | Surface Area Density [kg/m$^2$] | 2.0 |
| **Thermal Conductivity [W/(mK)]** | 0.167 | Thermal Conductivity [W/(mK)] | 2.1E-4 |

To preserve the current cabin layout, the fuel cell system and its BoP is placed in the tail cone. Since this system will occupy more space than the traditional APU, elongating the cabin has been identified as the most viable option. This modification will be factored into the aircraft-level analysis.

**Step 5: Thermal Management System Sizing and Modeling**
The thermal management system (TMS) plays a critical role in conditioning hydrogen and air to meet the temperature requirements of the PEMFC under operational conditions. The proposed TMS architecture (see Figure 6) includes three key heat exchangers, each serving a distinct function, and whose modeling approach is detailed in subsequent sections. First, a hydrogen boiler is used to bring liquid hydrogen to the working conditions of the PEMFC. To size the hydrogen boiler responsible for heating cryogenic hydrogen to the steady-state temperature required by the PEMFC, we assume an initial shell-and-tube heat exchanger geometry. Unlike TMS architectures in previous studies (Link et al., 2022), which rely on hot compressed air for hydrogen preheating, this method is not viable in our case during ground operations and low altitudes, where compressed air lacks sufficient thermal energy. Consequently, several heat sources were investigated in this study. The first one is to use bleed air, yet, in order to maintain engine performance this alternative was discarded. Alternatively,

® Cycom is a registered trademark of Syensqo SA/NV, Brussels, Belgium.
® Quest is a registered trademark of Quest Thermal Group, LLC, Arvada, Colorado.

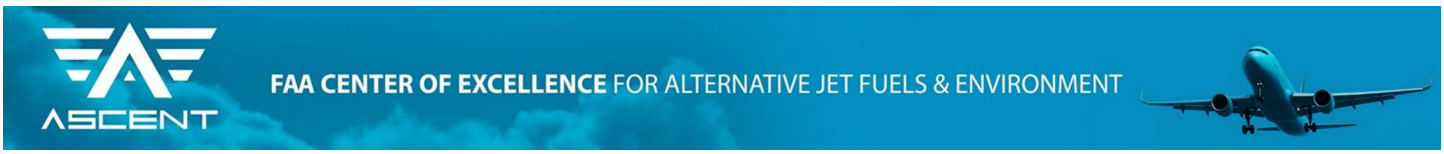

the heat up of cryogenic hydrogen to gas hydrogen could be performed by electric heaters alone, alimented by the PEMFC, yet this alternative increases the load on the PEMFC and increases the weight of the overall PEMFC subsystems. Consequently, the most viable alternative consists on using warm air from the stack heat exchanger for an initial heat up of the cryogenic hydrogen and adjusting the final temperature of gas hydrogen using electric heater (see Figure 13). Figure 14 depicts in blue the final hydrogen temperature after applying the first heat up and the red line depicts the required power to adjust the hydrogen temperature to the working temperature of the PEMFC through the mission.

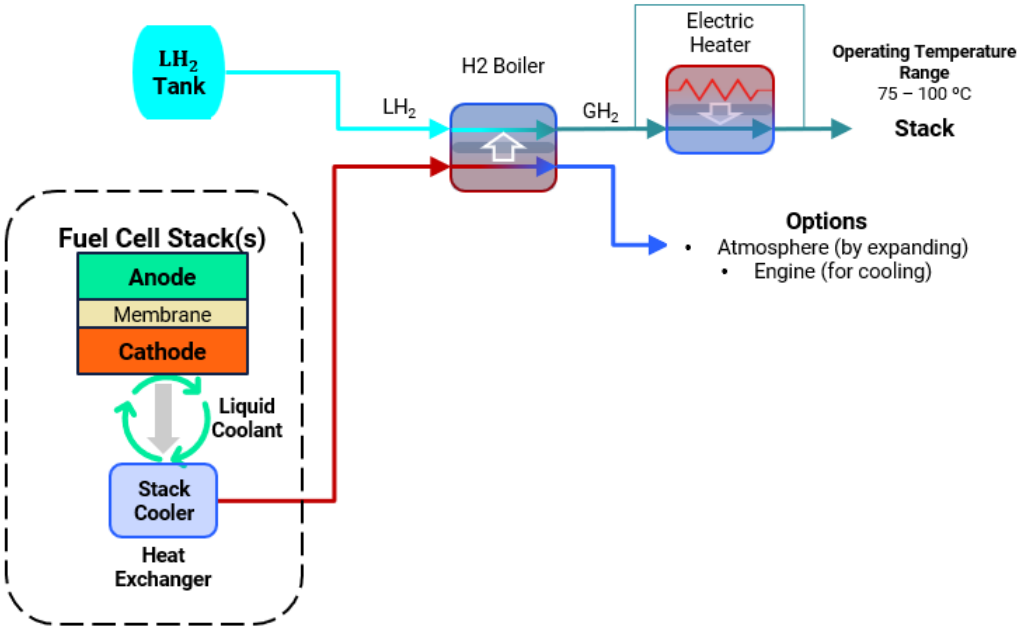


**Figure 13.** Hydrogen boiler architecture. $H_2$: hydrogen, $LH_2$: liquid hydrogen.

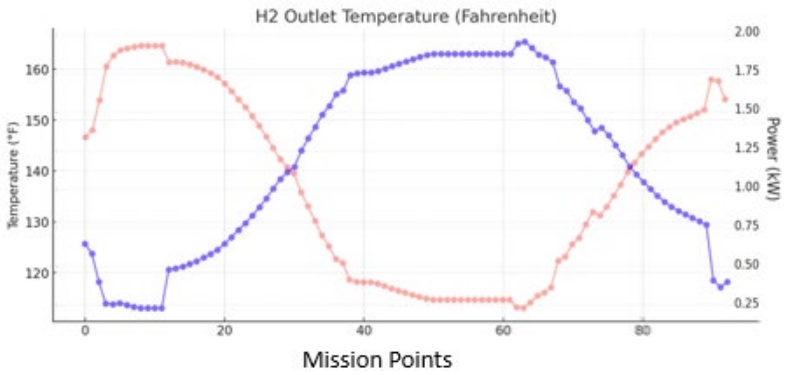


**Figure 14.** Hydrogen ($H_2$) temperature and required electric power for full heat up.

The sizing methodology is based on the effectiveness– number of transfer units (NTU) method. A thermal scaling parameter, referred to as the k factor, is applied to the initial geometry and dynamically updated at each iteration to rescale the heat exchanger. This iterative process continues until the hydrogen outlet temperature matches the PEMFC stack's target operating condition, ensuring effective thermal integration of the cryogenic hydrogen loop.

The second heat exchanger conditions the compressed air to bring it to the required PEMFC steady temperature. Many methods can be used to efficiently extract the waste heat of the PEMFC such as air cooling, heat spreaders or liquid cooling. Yet, for high waste heat (superior to 10kW), liquid cooling is a more efficient method (Baroutaji et al., 2021), consequently this method was considered in the current TMS architecture. The liquid cooling heat exchanger for the PEMFC stack is modeled as a finned flat tube exchanger, designed to manage the thermal load generated during PEMFC operation. The sizing process uses the effectiveness–NTU method in an iterative framework (Brooks & Mavris, 2021). Specifically, two pairs of dependent and independent variables are considered (see Table 5). As previously, the $k\ factor$ is dynamically updated in each iteration to rescale the heat exchanger geometry, starting from an initial assumed cube of 10 in. per side. Because the liquid coolant circuit operates in a closed loop, the target outlet temperature of the coolant is precomputed to match the inlet temperature, ensuring thermal equilibrium and effective heat rejection. Once convergence on the effectiveness and geometry is achieved, the solver computes the necessary ram air flow rate to meet the cooling requirement, ensuring the PEMFC stack operates within its designated temperature range for performance and durability. The algorithm used to size the PEMFC stack liquid heat exchanger is outlined in Table 6. The hot ram air exiting the heat exchanger will then be expelled and create a Meredith effect, where the exhausted hot air will provide an additional thrust (Frey et al., 2025). In order to integrate the air precooler in the global NPSS code, the modeling approach selected is presented in Figure 15. A bypass must be implemented to avoid an error from the solver. Indeed, during descent, the flow rate density increases and there is a limit altitude beneath which the mass flow rate is more than enough to cool down at 176°F. The NPSS solver tries to reduce the flow rate to meet the targeted temperature by giving negative values to the fan velocity. This leads to an error. The solution is therefore a bypass architecture with fixed rotating velocity for the fan and variation of bypass ratio.

**Table 5.** Considered dependent-independent variables.

| Dependent Variable | Independent Variable |
|---|---|
| **$k_{factor}$** | Target effectiveness |
| **Ram Air Flow Rate** | Liquid Coolant Outlet Temperature |

**Table 6.** Iterative sizing algorithm for liquid-cooled proton exchange membrane fuel cell (PEMFC) heat exchanger.

| Step | Description |
|---|---|
| 1 | Initialize geometry |
| 2 | Compute required incoming liquid temperature around the PEMFC to ensure steady stack temperature |
| 3 | repeat |
| 4 | Initialize ram air flow rate |
| 5 | repeat |
| 6 | Initialize ($k_{factor}$) |
| 7 | repeat |
| 8 | Initialize guess for air and liquid side temperatures |
| 9 | Compute liquid and air side characteristics using the effectiveness–NTU method |
| 10 | Update ($k_{factor}$) |
| 11 | until the effectiveness converges to the target |
| 12 | Update Hydrogen outlet temperature |
| 13 | until outlet Hydrogen temperature is at the stack steady temperature |

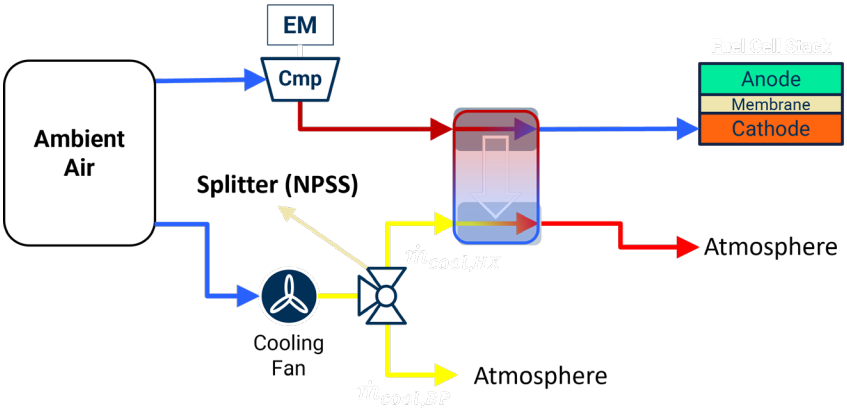


**Figure 15.** Air precooler modeling approach.

Finally, a third heat exchanger maintains the PEMFC stack temperature within safe operational limits to ensure system stability and fuel cell longevity. The air-air heat exchanger, also called air precooler, is used to cool down the compressed air to the operating temperature of the PEMFC stack. Several options can be considered to cool down the compressed air. First, hydrogen could be used as a liquid medium to remove the compressed air heat. Indeed, the hydrogen temperature is very low before the hydrogen boiler. This method has a double benefit: it cools down the air and heats up hydrogen. Thus, the hydrogen boiler can be downsized as the temperature raise needed is less important. It can ultimately lead to weight saving for the total system. However, this methodology presents a major drawback as the hydrogen mass flow rate is very low and probably not enough to achieve the required heat rejection. Another option would be to use hydrogen as a heat sink in addition to the air from ram air channels (Quaium et al., 2022). Yet this solution exacerbates the complexity of the architecture of the thermal management system. The most promising option would be to exploit only the ram air as the coolant medium and is further assessed below. In this solution, the air precooler receives hot pressurized air from the compressor outlet and uses ram air as a medium to extract the heat. The geometry used to model this heat exchanger is a finned flat tube exchanger, designed to manage the thermal load generated during the pressurization of ram air by the compressor. As for the PEMFC air-liquid heat exchanger, the sizing process uses the effectiveness–NTU method (Navarro & Cabezas-Gómez, 2006) in an iterative framework. The architecture of the system and the sizing methodology used are also similar to the PEMFC heat exchanger. The exact same pairs of dependent and independent variables are considered. Indeed, a *k factor* is implemented to match targeted effectiveness, and the ram air mass flow rate is varied to reach the correct temperature at the outlet of the heat exchanger (i.e., the stack temperature). The *k factor* is dynamically updated at each iteration to rescale the heat exchanger geometry, starting from an initial assumed cube of 20 in. per side. Once convergence on the effectiveness and geometry is achieved, the solver varies the ram air mass flow rate until the cooling requirement is satisfied. The new temperature of the compressed air at the outlet of the heat exchanger is recomputed at each iteration while ensuring thermal equilibrium and effective heat rejection. Finally, the necessary ram air flow rate to reach the steady stack temperature at the inlet of the stack is outputted. This ensures once again that the PEMFC stack operates within its designated temperature range for performance and durability.

## Milestones

- Imported the flight mission defined in EDS, used for aircraft sizing, into the NPSS environment. The manufacturer has also provided the average electrical power and bleed air requirements for each flight phase of the baseline aircraft. Step 1 has been completed.
- Established the fuel cell stack element for use in the NPSS environment, with both on-design and off-design capabilities. Step 2 has been completed.
- Established the fuel cell elements and their connections within the NPSS environment, and implemented weight-estimation models. Ongoing work focuses on refining the weight-estimation models to account for changes in the aircraft ducting system, such as additional air intakes, ducts, and nozzles. Step 3 is in progress.
- Implemented a cryogenic tank sizing function with the capability to handle several material types into the model. Step 4 has been completed.
- Developed thermal management system models and integrated the models into the NPSS environment and tested the models. Additional design alternatives are currently being explored. Step 5 is in progress.

## Major Accomplishments

- Added all major BoP components to a single modeling and simulation environment, tested, and used the components to create a suitable performance table for the aircraft mission analysis tool.
- Conducted a literature review, and identified the projected specific power and energy of the system's electrical components to support estimation of the system weight for the target year.

## Publications

Terzi, B., Decroix, J., Wattebled, L. A., Jazzini, A. S., Tai, J. C., & Mavris, D. (2025). Modeling Methodology for PEM Fuel Cells as Auxiliary Power Units in Aircraft Applications. In *AIAA AVIATION FORUM AND ASCEND 2025* (p. 3373).

## Outreach Efforts

- Scheduled and participated in monthly meetings with Gulfstream, Honeywell, and FAA to guide this research effort.
- Attended ASCENT biannual meetings.

## Awards

None.

## Student Involvement

This task involves four graduate students: Berkay Terzi (Ph.D. candidate), who worked on fuel cell stack modeling and integration of fuel cell components into the modeling environment; Jeremy Decroix (Ph.D. candidate), who worked on hydrogen tank sizing; Leo Wattebled (M.S. candidate), who worked on hydrogen preheater modeling; and Axel Jazzini (M.S. candidate) worked on compressor weight estimation and air precooler modeling.

## Plans for Next Period

- Refine some weight estimation models which are used in Task 2.
- Integrate the off-line PEMFC code into the EDS environment to enable seamless data transformation between them and centralize control from a single hub.

# Task 3 – Integrating Vehicle & PEMFC Models & Conducting Trade Studies

**Georgia Institute of Technology**

## Objective

The objective of Task 3 is to integrate the offline PEMFC code developed under Task 2 with the EDS environment to perform aircraft-level assessments and conduct feasibility studies for the proposed fuel-cell system.

## Research Approach

As described in Task 2, the proposed fuel-cell system must satisfy three primary objectives: (1) supplying electrical power to aircraft subsystems, (2) providing pressurized air for the ECS, and (3) enabling independent engine start without external power sources. In the baseline aircraft, the conventional gas-turbine APU fulfills these requirements by delivering backup AC power up to 20,000 feet, supplying in-flight bleed air for air-conditioning up to 15,000 feet, and providing pneumatic power for engine start. These functions are achieved through extracting of shaft power and bleed air from the engine compressor (Honeywell, 2008).

In the proposed architecture, however, the fuel-cell system will supply continuous electrical power and pressurized air for the ECS throughout the entire flight, thereby reducing Jet-A fuel consumption and overall emissions. In Task 3, the fuel-cell system weight will be estimated using the modeling environment developed in Task 2, and aircraft-level weight-balance implications will be assessed in EDS. The overarching objective is to perform these analyses within a unified modeling and simulation framework. Using this simulation framework will also streamline the process and enable possible parametric studies.

**Step 1: PEMFC System Weight Estimation**

One of the main parameters for sizing a PEMFC system to meet target performance is the power demand of the aircraft subsystems. Because business-jet designs vary more widely than those of commercial transport aircraft, the subsystem

power demand which is provided directly by the manufacturer rather than estimated using generalized equations will be used for sizing the system.

The power demand of the electric ECS is another key factor in the sizing process. Since this project focuses on fuel cells, the ECS packs themselves will not be modeled; instead, their power consumption will be included within the overall aircraft subsystem loads. However, the cabin air compressors and their driving electric motors will be sized to deliver the required discharge pressure while providing the necessary fresh-air flow rate to the cabin. Their resulting power consumption will be quantified and will play a significant role in the overall sizing process. The selection of the thermal-conditioning pack cycle type, as shown in Figure 12, is also an important consideration, since discharge pressure directly influences power consumption. Based on aircraft manufacturer feedback, the discharge pressure associated with the preferred thermal-conditioning pack will be used.

Once system performance, including parasitic power consumption, has been defined, the weights and volumes of the components must be estimated for aircraft-level assessment. Because implementing such a system is a long-term effort, technology-projection studies are required to establish future assumptions for component-specific power, volume, and efficiency. Several references provided in Task 2 already contain useful projected specific-power data for certain components (Aerospace Technology Institute, 2022; Pastra et al., 2022; Hall et al., 2022; Tiede et al., 2022; Schröder et al., 2021). Having projected values across multiple future time horizons also enables identification of the breakeven point at which the fuel-cell system becomes competitive in terms of weight. Ongoing work includes expanding the set of technology-assumption studies and identifying current industry manufacturers of fuel cells and fuel-cell components. In parallel, the system layout will also be defined to support accurate estimation of ducting and cable weights, as well as any internal or external modifications to the aircraft required to integrate the system into the aircraft.

**Step 2: Aircraft Level Assessment of the New System**

For seamless integration of the PEMFC modeling environment into EDS, a performance table is generated by running the model in off-design mode at each point in the flight envelope. This table contains the hydrogen consumption rate, ram drag, and the thrust produced by the expansion of warm, pressurized air. However, the aircraft mission analysis software FLOPS cannot simultaneously utilize two engine decks within the same mission segment. In this study, both the conventional engine deck and the PEMFC performance table are required to conduct the analysis. To address this limitation, a combined engine deck is created by merging the conventional engine deck with the PEMFC performance table, following the process outlined in Figure 16.

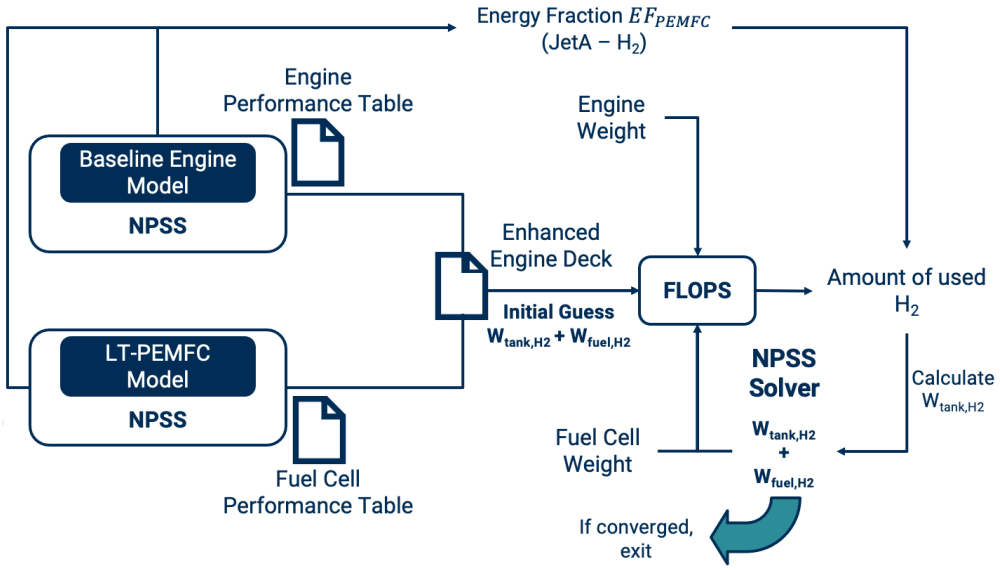


**Figure 16.** Aircraft modeling environment integration process.

The following performance metrics are modified to account for hydrogen consumption, PEMFC-generated thrust and the drag penalty introduced by the PEMFC system integration:

$$\dot{m}_{Fuel} = \dot{m}_{kerosene} + \dot{m}_{hydrogen} \quad \text{(Eq. 10)}$$

$$F_g = F_{g,Engine} + F_{g,PEMFC} \quad \text{(Eq. 11)}$$

$$D_{ram} = D_{ram,Engine} + D_{ram,PEMFC} \quad \text{(Eq. 12)}$$

$$TSFC = \frac{\dot{m}_{kerosene}+\dot{m}_{hydrogen}}{(F_{g,Engine}+F_{g,PEMFC})-(D_{ram,Engine}+D_{ram,PEMFC})} \quad \text{(Eq. 13)}$$

To track the relative usage of kerosene and hydrogen throughout the mission the energy fraction (EF) metric is defined as:

$$EF = \frac{\dot{m}_{hydrogen}}{\dot{m}_{kerosene}+\dot{m}_{hydrogen}} \quad \text{(Eq. 14)}$$

The resulting combined dataset is then imported into FLOPS within the EDS environment to enable accurate mission analysis and determine the required liquid hydrogen tank capacity.

In designing a new aircraft power system, it is also essential to consider emergency scenarios that require redundancy. In the proposed configuration, the fuel cell system serves as the primary power source under the revised mission profile. However, one of the original engine-mounted generators may be retained—potentially in a downsized form—to provide a backup power source in the event of a fuel-cell system failure. This ensures continued electrical power supply to critical subsystems, thereby maintaining operational safety and system reliability.

To support a fair comparison against the PEMFC-powered configuration, the notional calibrated aircraft baseline is additionally resized to reflect the fuel consumption that would result if the conventional APU were operated throughout the entire mission. This produces a more representative reference configuration, since the PEMFC system is designed to supply electrical power and bleed air to the ECS continuously for the full mission duration.

For the aircraft-level system assessment, two evaluation pathways are considered. The first is a retrofit analysis, in which the aircraft geometry remains unchanged; in this case, the comparison can be conducted under either fixed-payload or fixed-range assumptions. The second pathway is a resize analysis, where the fuselage is extended to accommodate PEMFC subsystem integration—most notably the cryogenic hydrogen tank. Across both approaches, key metrics such as weight penalties or benefits, fuel savings, emissions reductions, and payload–range impacts are systematically tracked to quantify the overall aircraft-level performance of PEMFC integration.

## Milestone

Ran two modeling and simulation environments separately to generate interim results, and to demonstrate their usefulness. Once the fuel cell model is finalized, efforts will be focused on integrating these environments. Steps 1 and 2 are in progress.

## Major Accomplishments

Examined the weight effects at the aircraft level are examined using the interim results from the fuel cell sizing tool.

## Outreach Efforts

- Scheduled and participated in monthly meetings with Gulfstream, Honeywell, and FAA to guide this research effort.
- Attended ASCENT biannual meetings.

## Publications

None.

## Awards
None.

## Student Involvement
This task involves two graduate students: Berkay Terzi (Ph.D. candidate), who worked on the PEMFC system weight estimation; Jeremy Decroix (Ph.D. candidate), who worked on the aircraft modeling environment integration process and the aircraft system-level performance assessment.

## Plans for Next Period
- Integrate the off-line PEMFC code into the EDS environment to enable seamless data transformation between them and centralize control from a single hub.
- Conduct more comprehensive design studies by expanding the design space following the integration of the two environments.
- Evaluate the volumetric impact of the new system on the aircraft.

## References

Aerospace Technology Institute. (2022). Fuel Cells Roadmap Report (FZO-PPN-COM-0033). https://www.ati.org.uk/wp-content/uploads/2022/03/FZO-PPN-COM-0033-Fuel-Cells-Roadmap-Report.pdf

Bargal, M. H., Abdelkareem, M. A., Tao, Q., Li, J., Shi, J., & Wang, Y. (2020). Liquid Cooling Techniques in Proton Exchange Membrane Fuel Cell Stacks: A Detailed Survey. Alexandria Engineering Journal, 59(2), 635–655. https://doi.org/10.1016/j.aej.2020.02.005

Baroutaji, A., Arjunan, A., Ramadan, M., Robinson, J., Alaswad, A., Abdelkareem, M. A., & Olabi, A.-G. (2021). Advancements and prospects of thermal management and waste heat recovery of PEMFC. *International Journal of Thermofluids, 9*, 100064. https://doi.org/10.1016/j.ijft.2021.100064

Brooks, J., & Mavris, D. N. (2021). Compact heat exchanger sizing and weight estimation. In *AIAA Propulsion and Energy 2021 Forum* (p. 3711). https://doi.org/10.2514/6.2021-3711

Cai, Y. (2023). Multi-mission sizing and analysis framework for aircraft and subsystem architectures with electrified propulsion systems [Doctoral dissertation, Georgia Institute of Technology].

Campbell, K., & Talbert, J. E. (1945). *Some advantages and limitations of centrifugal and axial aircraft compressors," SAE Transactions* (pp. 607–620). SAE Technical Paper 450224. https://doi.org/10.4271/450224

Chang, Y., Qin, Y., Yin, Y., Zhang, J., & Li, X. (2018). Humidification Strategy for Polymer Electrolyte Membrane Fuel Cells–A Review. *Applied energy, 230*, 643–662. https://doi.org/10.1016/j.apenergy.2018.08.125

Daggett, D., Eelman, S., & Kristiansson, G. (2003). Fuel cell APU. In *AIAA International Air and Space Symposium and Exposition: The Next 100 Years* (p. 2660).

Datta, A. (2021). PEM Fuel Cell Model for Conceptual Design of Hydrogen eVTOL Aircraft. National Aeronautics and Space Administration. https://ntrs.nasa.gov/citations/20210000284

EASA. (2020). *Type Certificate Data Sheet No. EASA.IM.A.348 for Gulfstream G280*. European Union Aviation Safety Agency. https://www.easa.europa.eu/en/document-library/type-certificates/noise/easaima348-gulfstream-lp-g280

FAA. (1996). AC 25-20 - Pressurization, Ventilation and Oxygen Systems Assessment for Subsonic Flight Including High Altitude Operation. Federal Aviation Administration. https://www.faa.gov/regulations_policies/advisory_circulars/index.cfm/go/document.information/documentid/22648

Frey, A. C., Stonham, J., Bosak, D., Sangan, C. M., & Pountney, O. J. (2025). Radiators in fuel cell powered aircraft: the effect of heat rejection on drag. *Applied Thermal Engineering, 274*, 126697. https://doi.org/10.1016/j.applthermaleng.2025.126697

Hall, C., Pastra, C. L., Burrell, A., Gladin, J., & Mavris, D. N. (2022). Projecting Power Converter Specific Power through 2050 for Aerospace Applications. *2022 IEEE/AIAA Transportation Electrification Conference and Electric Aircraft Technologies Symposium (ITEC+EATS)*, Anaheim, California (pp. 760–765). https://doi.org/10.1109/ITEC53557.2022.9813991

Honeywell. (n.d.). *Honeywell 36-150 Ported Shroud APU, Redimec*. https://www.redimec.com.ar/contenido/productos/pdf/1425325504_1.pdf (accessed November 21, 2024)

Johnson, W., Baltman, E., & Koci, F. (2024). Assessment of Insulation Systems for Aircraft Liquid Hydrogen Tanks. *IOP Conference Series: Materials Science and Engineering, 1301*, 012062. https://doi.org/10.1088/1757-899X/1301/1/012062

Link, A., Ludowicy, J., & Staggat, M. (2022, September 4-9). Assessment of a serial cooling concept for htpem fuel cell systems for aviation applications [Conference paper]. 33rd Congress of the International Council of the Aeronautical Sciences – ICAS 2022, Stockholm, Sweden. https://elib.dlr.de/188369/1/ICAS2022_0456_paper.pdf

MANN+HUMMEL. (n.d.). Water Separator- Fuel Cells. https://shop.mann-hummel.com/en/e-mobility/fuel-cells 1231/water-separator.html (accessed May 14, 2025).

MicroPump, Inc. (2025). EagleDrive DEE/LE. https://micropump.com/products/drives/eagledrive-deele?language_code=en, 2025

Navarro, H. A., & Cabezas-Gómez, L. C. (2006). Effectiveness-NTU computation with a mathematical model for cross-flow heat exchangers. *Brazilian Journal of Chemical Engineering, 24*(04), 509-521.

O'Hayre, R., Cha, S.-W., Colella, W., & Prinz, F. B. (2016). *Fuel Cell Fundamentals*. John Wiley & Sons. https://doi.org/10.1002/9781119191766

Pastra, C. L., Hall, C., Cinar, G., Gladin, J., & Mavris, D. N. (2022). Specific Power and Efficiency Projections of Electric Machines and Circuit Protection Exploration for Aircraft Applications. *2022 IEEE/AIAA Transportation Electrification Conference and Electric Aircraft Technologies Symposium (ITEC+EATS)*, Anaheim, California (pp. 766–771). https://doi.org/10.1109/ITEC53557.2022.9813927

Quaium, F., Bielsky, T., & Thielecke, F. (2022). *Fuel Cell Cooling System Design for Hydrogen-Powered Concept Aircraft*. Deutsche Gesellschaft für Luft- und Raumfahrt - Lilienthal-Oberth e.V. (Text). https://doi.org/10.25967/570127

Rosero, J., Ortega, J., Aldabas, E., & Romeral, L. (2007). Moving towards a more electric aircraft. *IEEE Aerospace and Electronic Systems Magazine, 22*(3), 3–9. https://doi.org/10.1109/MAES.2007.340500

Rotrex Fuel Cell Compressors. (2025). Fuel Cell Compressors. https://rotrex-fuel-cell-compressor.com/fuel-cell-compressors/

Schröder, M., Becker, F., Kallo, J., & Gentner, C. (2021). Optimal operating conditions of PEM fuel cells in commercial aircraft. *International Journal of Hydrogen Energy, 46*(66), 33218–33240. https://doi.org/10.1016/j.ijhydene.2021.07.099

Smith, P. J., Bennett, W. R., Jakupca, I. J., Gilligan, R. P., & Edwards, L. G. (2021). *Proton Exchange Membrane Fuel Cell Transient Load Response*. National Aeronautics and Space Administration. https://ntrs.nasa.gov/citations/20210018094

Tagge, G., Irish, L., & Bailey, A. R. (1985). *Systems study for an Integrated Digital-Electric Aircraft (IDEA).* National Aeronautics and Space Administration. https://ntrs.nasa.gov/citations/19850007405

Tiede, B., O'Meara, C., & Jansen, R. (2022). Battery key performance projections based on historical trends and chemistries," *2022 IEEE/AIAA Transportation Electrification Conference and Electric Aircraft Technologies Symposium (ITEC+EATS)*, Anaheim, California (pp. 754–759). https://doi.org/10.1109/ITEC53557. 2022.9814008

Voth, V., Lübbe, S. M., & Bertram, O. (2024). Estimating Aircraft Power Requirements: A Study of Electrical Power Demand Across Various Aircraft Models and Flight Phases. *Aerospace, 11*(12), 958. https://doi.org/10.3390/aerospace11120958

Willich, C., Tomaszewski, A., Henke, M., Friedrich, K. A., & Kallo, J. (2014). Temperature effect due to internal reforming in pressurized SOFC. *Journal of The Electrochemical Society, 161*(5), F674. https://doi.org/10.1149/2.075405jes

Willich, C., Frank, D., Graf, T., Wazlawik, S., Brandao, S., & Bauer, C. (2024). High-Altitude Operation of a Commercial 100 kW PEMFuel Cell System. Energies, 17(24), 6903. https://doi.org/10.3390/en17246309